3D Fluid Stress Field Reconstruction from Flow Birefringence: Physics-Informed Convolutional Encoder-Decoder Approach

D Igarashi[1], S Kumagai[1], Y Yokoyama[1], Y Jingzu[1], M Horie[2], Y Tagawa[1]

[1]*Department of Mechanical Systems Engineering, Tokyo University of Agriculture and Technology*

[2]*RICOS Co. Ltd.*

Keywords: Physics-informed neural network, Convolutional Encoder-Decoder, Fluid stress field, Photoelasticity

Abstract. Measuring the stress field in complex fluid flows is essential for a wide range of applications. However, calculating the stress field in such fluids poses a significant challenge, as the constitutive equation that links the velocity field to the stress field remains elusive. To address this challenge, we have introduced a machine learning-based photoelasticity approach for stress field measurement. In this study, we reconstructed the three-dimensional stress field from two-dimensional images of flow birefringence, which directly reflects the stress distribution. The birefringence, characterized by optical retardation and fluid particle orientation, was experimentally captured using a polarization camera in a rectangular channel. This reconstruction is achieved through our originally developed 3D Physics-Informed Convolutional Encoder-Decoder (PICED) model—an Encoder-Decoder architecture that integrates a Convolutional Neural Network (CNN) with a Physics-Informed Neural Network (PINN), embedding physical equations within the loss function. The results demonstrate that our model achieves a degree of accuracy in predicting the three-dimensional stress field for interpolated data. These findings underscore the efficacy of incorporating physical equations into machine learning models, enabling more precise predictions compared to approaches relying solely on data error minimization. This model holds promise as a groundbreaking approach for three-dimensional stress field reconstruction.

1. Introduction

The fluid stress field is typically determined by applying the constitutive equation to the velocity distribution. Therefore, computing the stress field from the velocity field becomes a significant challenge for complex fluids where the constitutive equation is unclear. Blood serves as a prime example of such a complex fluid. Previous research has aimed to uncover the causes of cerebral aneurysms—bumps in blood vessels—by employing numerical simulations to analyze the stress fields of blood flow. However, the cause remains unresolved due to the limitations and incompleteness of the mathematical model[(1)]. For the completely novel approach to measure the stress fields, Muto et al. achieved the groundbreaking visualization of the optical phase difference (retardation) Δ [m] and its orientation φ [rad] induced by flow birefringence with the use of a polarization camera[(2)]. Retardation refers to the deviation of light waves due to stress-induced strain and orientation indicates the direction of the principal stress. These values are denoted as

$$\Delta^{(i)} = Cd\sqrt{(\sigma_{xx}^{(i)} - \sigma_{yy}^{(i)})^2 + 4(\sigma_{xy}^{(i)})^2}, \tag{1}$$

$$\varphi^{(i)} = \frac{1}{2}\tan^{-1}\frac{2\sigma_{xy}^{(i)}}{\sigma_{xx}^{(i)} - \sigma_{yy}^{(i)}}, \tag{2}$$

where the superscript (i) denotes the i-th thin plate obtained by slicing the measurement object along the optical axis. Here, C represents the stress-optic coefficient, d is the thickness of a thin plate, and σ_{xx}, σ_{xy}, and σ_{yy} are the stress components in the Cartesian coordinate system[(3)]. Although visualizing retardation and orientation facilitates stress field measurement, the data acquired by the polarization camera is an integrated value, computed through sophisticated matrix calculations across multiple plates. Furthermore, reconstructing stress fields involves tackling a complex nonlinear problem.

This study focused on leveraging machine learning to address nonlinear challenges. In recent years, machine learning-driven 3D image reconstruction has not only advanced within the realm of fluid

dynamics but has also made notable progress across a wide range of other disciplines[4]. This study aims to develop a machine-learning model capable of reconstructing a three-dimensional stress tensor field from two-dimensional integral images of retardation and orientation. Rather than relying on conventional machine learning approaches that overlook physical principles, this study leverages a Physics-Informed Neural Network (PINN), a neural network framework that incorporates governing physical equations[5]. This paper presents the reconstruction of stress fields for rectangular pipe flows across varying aspect ratios using supervised learning.

2. Methodology

Figure 1a illustrates the experimental setup. Light from the source traverses a circular polarizer and the measurement object before reaching a high-speed polarization camera, enabling the measurement of the fluid's birefringence. The measurements were conducted using two types of rectangular pipes with aspect ratios $w/d = 1.0$ and $w/d = 3.0$, as shown in figure 1a. A CNC-HS-FD solution (1.0 wt%), which is a photoelastic fluid, is flowed as the working fluid. Photoelastic fluids induce birefringence in the fluid, allowing measurement of retardation and orientation. Figure 1b presents the (i) retardation and (ii) orientation distributions obtained from the experiment. The flow rate, Q, was varied between 5 and 80 mL/min, and a total of 19 different conditions were tested.

To reduce computation time for machine learning, all images are resized to 64 × 64 pixels using the bicubic interpolation method. In addition, to minimize the influence of experimental errors, time averages were calculated by acquiring five images for each condition. In this study, five datasets with $w/d = 1.0$ and $Q = 40$ mL/min were designated as test data, while the remaining 90 datasets were utilized for training. The theoretical solutions of the Newtonian fluid laminar flow in a rectangular pipe were used as the stress distributions for the true values of the supervised learning. The stress tensor components in rectangular pipe flow adhere to the following equation:

$$\boldsymbol{\sigma} = \begin{bmatrix} \sigma_{xx} & \sigma_{xy} & \sigma_{xz} \\ \sigma_{yx} & \sigma_{yy} & \sigma_{yz} \\ \sigma_{zx} & \sigma_{zy} & \sigma_{zz} \end{bmatrix} = \begin{bmatrix} -p & \sigma_{xy} & \sigma_{xz} \\ \sigma_{xy} & -p & 0 \\ \sigma_{xz} & 0 & -p \end{bmatrix}. \tag{3}$$

where p is atmospheric pressure. Thus, σ_{xy} and σ_{xz}, which vary between datasets, were used in the analysis. Based on this, machine learning was conducted using the two-dimensional distributions of retardation and orientation as input, and the three-dimensional stress tensor distribution as output.

The 3D Physics-Informed Convolutional Encoder-Decoder (PICED) model, shown in figure 2, was employed as the machine learning model. This model is a three-dimensional image generation architecture capable of reconstructing a three-dimensional stress field from two-dimensional input images of retardation and orientation[6]. Furthermore, by incorporating physical equations into the loss

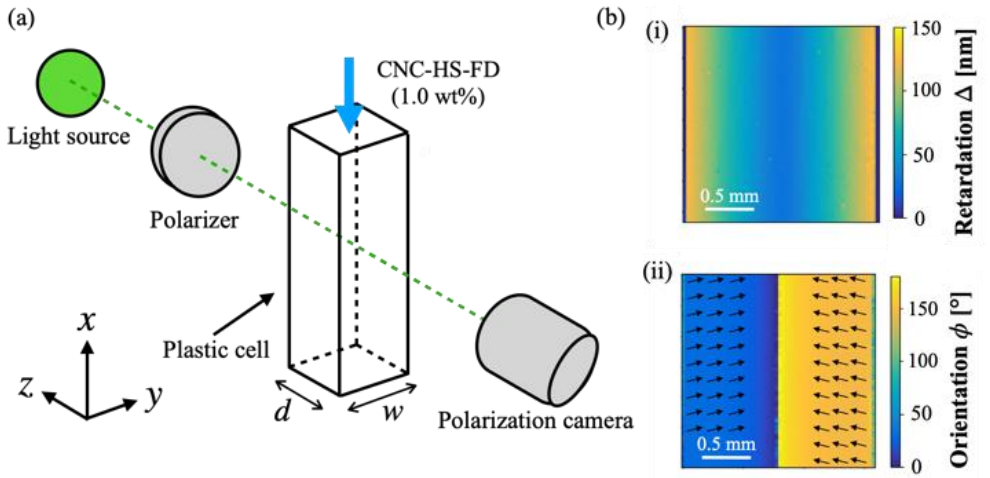

Figure 1 (a) Illustration of the experimental setup and (b) representative images showcasing (i) retardation and (ii) orientation captured from the experiment ($Q = 40$ mL/min).

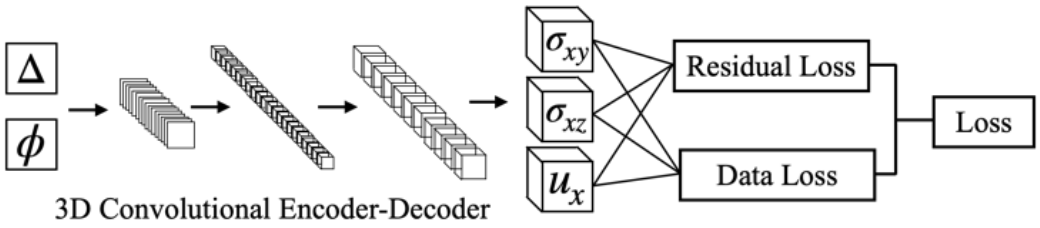

Figure 2 3D Physics-Informed Convolutional Encoder-Decoder (PICED) as the machine learning model.

function, the model can make predictions that account for underlying physical phenomena. In this study, the Cauchy equation and the continuity equation were employed as the governing physical equations. The velocity in the x-direction, u_x, is necessary for the physical equations, and thus, the velocity is also incorporated into the output. Note that the true values of the velocity distribution are derived from the theoretical solution. Let L_{data} represent the data error, calculated using the mean squared error (MSE), L_{N} the residual derived from the Cauchy equation, and L_{C} the residual from the continuity equation. The overall loss function, L_{total}, is defined by the following equation:

$$L_{total} = L_{\text{data}} + ß_1 L_{\text{N}} + ß_2 L_{\text{C}}, \tag{4}$$

where λ_1 and λ_2 are fitting parameters, and $\lambda_1 = 10^{-4}$ and $\lambda_2 = 1.0$. Furthermore, L_{data}, L_{N} and L_{C} can be expressed by the following equations:

$$L_{\text{data}} = \frac{1}{N}\sum^{N}(\sigma_{xy}^{a} - \sigma_{xy}^{p})^2 + \frac{1}{N}\sum^{N}(\sigma_{xz}^{a} - \sigma_{xz}^{p})^2 + \frac{1}{N}\sum^{N}(u_x^{a} - u_x^{p})^2, \tag{5}$$

$$L_{\text{N}} = \frac{1}{N}\sum^{N}\left[\frac{1}{\rho}\left(\frac{\partial\sigma_{xy}^{p}}{\partial y} + \frac{\partial\sigma_{xz}^{p}}{\partial z}\right) - u_x^{p}\frac{\partial u_x^{p}}{\partial x}\right]^2, \quad L_{\text{C}} = \frac{1}{N}\sum^{N}\left(\frac{\partial u_x^{p}}{\partial x}\right)^2, \tag{6}$$

where N is the number of data points in one image, the superscript "p" is the predicted value, and "a" is the true value. The central difference method was employed for the differential calculations. The computations were carried out in parallel (data parallel) using 4 GPUs.

3. Results & Discussion

Figure 3 presents the results of reconstructing the theoretical solution (Theory), representing the true values, alongside the stress and velocity fields predicted by PICED.

The reconstruction outcomes using only MSE as the loss function (CNN) are also displayed for comparison.

These results demonstrate that CNN provides more accurate predictions for both stress and velocity fields.

Specifically, the mean absolute errors (MAEs) for PICED and CNN when compared to the theoretical solution are 0.105 and 0.849 for σ_{xy}, 0.127 and 0.087 for σ_{xz}, and 4.93×10^{-2} and 1.55×10^{-2} for u_{x}, respectively, highlighting the superior accuracy of CNN. On the other hand, all methods successfully predicted the stress field with a reasonable degree of accuracy, suggesting that these models can effectively reconstruct the three-dimensional stress field for rectangular pipe flows across different aspect ratios. To further evaluate the accuracy of the machine learning models, figure 4 presents the predicted values of stress and velocity along each axis for the center line (Lines 1-4) of each cross-section, as shown in figure 3, for both PICED and CNN. Numerical simulation results for Q = 30 and 50 mL/min, which have stress and velocity values close to the test data for Q = 40 mL/min, are also included in the same figure.

Figure 4a demonstrates that both PICED and CNN can predict σ_{xy} with high accuracy around y = 5-30 pixels, while PICED yields predictions closer to the theoretical values for y = 30-60 pixels. However, near the inlet and outlet (i.e., y = 1-4, 61-64 pixels), PICED predictions become large outliers, whereas CNN predictions are closer to the theoretical values. This discrepancy is likely attributed to PICED's use of the central difference method for solving the physical equations, leading to difficulties near the

boundary of the computational domain. The reason CNN appears more accurate in the results shown in figure 3 and in the MAE calculation is that PICED's predictions near the boundary were less precise. This suggests that incorporating boundary conditions is crucial to improving prediction accuracy near the domain boundaries. A similar trend is observed for σ_{xz} with respect to the position in the z-direction (figure 4b). Despite introducing certain errors, CNN successfully predicted the interpolated stress values (and velocity values) not present in the training set with a reasonable degree of accuracy.

On the other hand, as shown in figure 4c, PICED demonstrates less accuracy for the velocity values in relation to the position along the y-direction. This inconsistency is likely due to the error introduced by the continuity equation and the mismatch with the correct image. However, as illustrated in figure 4d, along the x-direction, which corresponds to the flow direction, PICED successfully mitigates abrupt changes between consecutive points and learns to better satisfy the continuity equation. Thus, it is essential to reconsider the fitting parameter λ_2 to reduce the error between the correct image and the predicted image in the y-direction while still satisfying the continuity equation along the flow direction.

In addition, to explore the influence of the physical equations, we examined the values of L_N and L_C from Eq. (6). For PICED, $L_N = 1.89 \times 10^{-2}$ and $L_C = 1.85 \times 10^{-6}$, while for CNN, $L_N = 0.484$ and $L_C = 1.26 \times 10^{-5}$. These results suggest that PICED more accurately predicts the physical equations than CNN.

The results above indicate that machine learning can successfully predict the stress distribution of interpolated data with varying aspect ratios using two-dimensional images integrated with retardation and orientation. Furthermore, the findings suggest that PICED is a machine-learning model capable of incorporating physical equations.

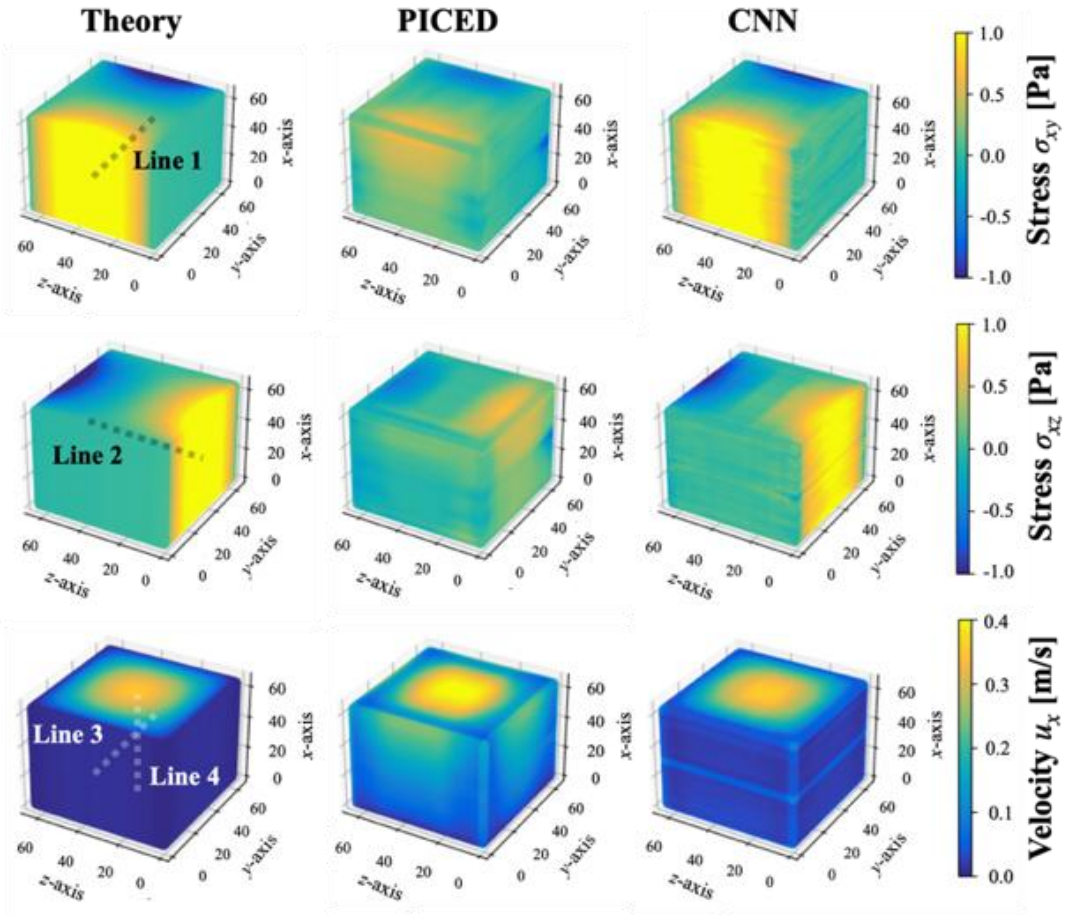

Figure 3 Stress and velocity distributions: theoretical values, prediction values of PICED and CNN.

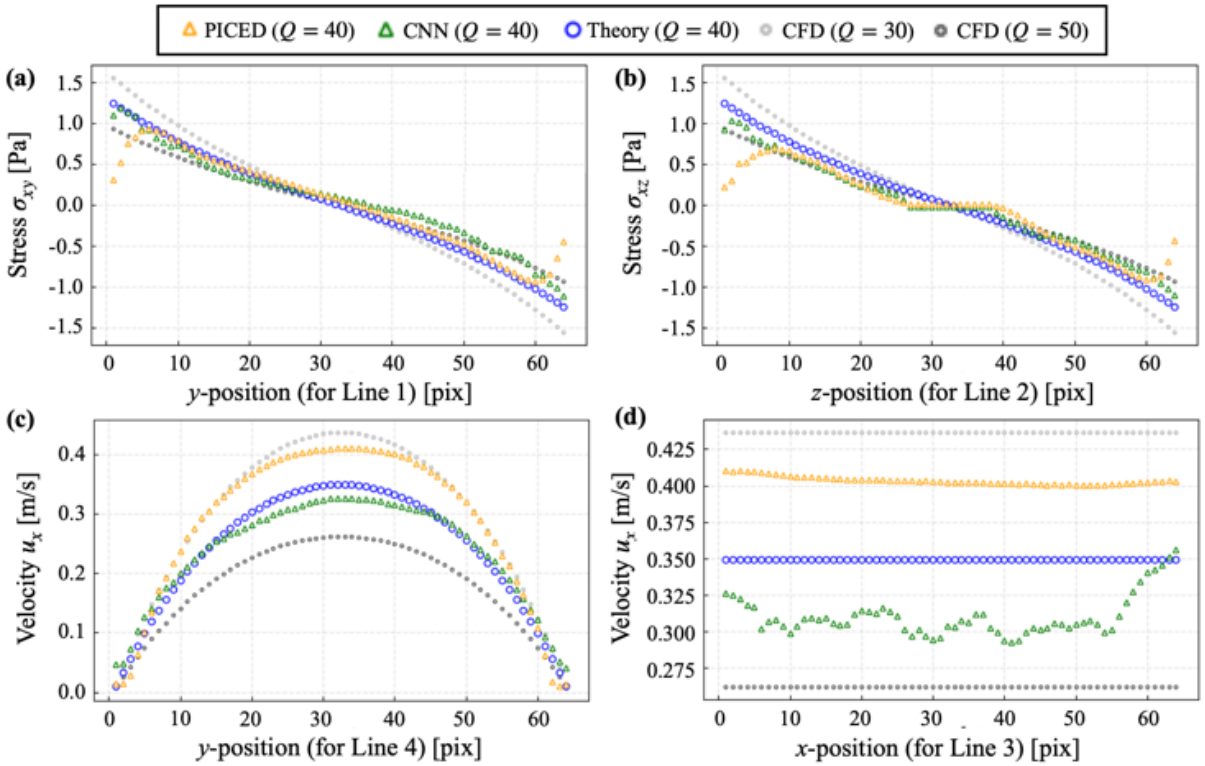

Figure 4 Stress and velocity values for each axis.

4. Conclusion

This study aims to develop a machine learning model capable of reconstructing a three-dimensional stress field from a two-dimensional integrated image of retardation and orientation captured by a high-speed polarization camera. In this paper, machine learning was implemented using a 3D Physics-Informed Convolutional Encoder-Decoder (PICED) and CNN to analyze a rectangular pipe channel with varying aspect ratios. As a result, the stress distribution of interpolated data was successfully predicted with notable accuracy. Predicting channels with different aspect ratios enables the estimation of values along the integration direction, providing key insights for extending predictions to more complex channel geometries. As for PICED, it learned to satisfy the Cauchy equation and the continuity equation, suggesting that it is a model that can take the physical equations into account better than CNN. However, PICED currently demonstrates lower accuracy than CNN near walls and in certain regions, and we aim to refine the model to enhance its precision in future work. Moving forward, we strive to predict three-dimensional flow by utilizing images captured from multiple directions. Building on this plan, our ultimate goal is to reconstruct three-dimensional fluid stress fields in complex geometries through machine learning.

5. References

[1] Shojima, M., Oshima, M., Takagi, K., Torii, R., Hayakawa, M., Katada, K., & Kirino, T. 'Magnitude and role of wall shear stress on cerebral aneurysm: computational fluid dynamic study of 20 middle cerebral artery aneurysms', Stroke, https://doi.org/10.1161/01.STR.0000144648.89172.0f

[2] Muto, M., Worby, W. K. A., Nakamine, K., Yokoyama, Y., & Tagawa, Y. 'Non-Contact And Non-Steady Rheo-Optical Measurement Of Hydrodynamic Stress Fields Inside A Cylindrical Tube', Proceedings of the International Symposium on the Application of Laser and Imaging Techniques to Fluid Mechanics, July 2022

[3] Nakamine, K., Yokoyama, Y., Worby, W., Muto, M., & Tagawa, Y. 'Integrated photoelasticity measurements of a three-dimensional laminar flow: Second-order stress terms in the stress-optic law', Optica Open, https://doi.org/10.1364/opticaopen.21967049.v1

[4] Mescheder, L., Oechsle, M., Niemeyer, M., Nowozin, S., & Geiger, A. 'Occupancy networks: Learning

3d reconstruction in function space', Proceedings of the IEEE/CVF conference on computer vision and pattern recognition, 2019
[5] Karniadakis, G. E., Kevrekidis, I. G., Lu, L., Perdikaris, P., Wang, S., & Yang, L. 'Physics-informed machine learning.', Nature Reviews Physics, https://doi.org/10.1038/s42254-021-00314-5
[6] Shan, H., Zhang, Y., Yang, Q., Kruger, U., Kalra, M. K., Sun, L., & Wang, G. '3-D convolutional encoder-decoder network for low-dose CT via transfer learning from a 2-D trained network', IEEE transactions on medical imaging, 10.1109/TMI.2018.2832217